*International Journal of Advanced Engineering, Management and Science (IJAEMS)*
*ISSN: 2454-1311*
*Vol-7, Issue-3; Mar, 2021*
*Journal Home Page Available: https://ijaems.com/*
*Journal DOI: https://dx.doi.org/10.22161/ijaems*
*Article DOI: https://dx.doi.org/10.22161/ijaems.73.5*

# Model Predictive Control for Three-phase Grid-Connected Inverters

Quang-Tho Tran*, Thanh-Lam Le, Huu-Lam Ho, Phu-Cuong Nguyen, Quang-Hieu Nguyen, and Van-Hien Truong

Faculty of Electrical and Electronics Engineering, HCM city University of Technology and Education, Hochiminh city, Vietnam
*Corresponding author

Received: 09 Dec 2020; Received in revised form: 03 Feb 2021; Accepted: 20 Feb 2021; Available online: 15 Mar 2021


***Abstract***— *Demands of renewable energy are increasing due to its effectiveness and sustainability. However, this energy source depends much on the weather and is unstable. Therefore, it needs to be connected to the power network via grid-connected inverters using power electronics devices. The power quality of inverter outputs depends much on the control strategy and modulation. The conventional control methods such as the proportional-integral (PI) and proportional resonance (PR) use the control loops and depend on the controller coefficients. The hysteresis current control method offers the best dynamic response. However, its switching frequency is very difficult to control. This paper presents a method basing on the model predictive control. In the proposed method, the inverter switching states are optimally chosen to minimize the cost function. This helps inverters reduce the switching counts while ensuring the low output harmonics. Thus, this can help inverters decrease the switching loss. The simulation results on Matlab/Simulink have validated the effectiveness of the proposed control method compared with that of the hysteresis current one.*

***Keywords***— ***Grid-connected inverters, current harmonics, PR control, hysteresis control, model predictive control.***

## I. INTRODUCTION

The electric systems using renewable energy through the three-phase grid-connected inverters are increasing [1]. The power quality of inverter outputs depends much on the control strategies. There are many types of current controllers used for the three-phase grid-connected inverters such as PI, PR, and hysteresis current (HC). The PI and PR controllers are often used very popular in the control of grid-connected inverters due to their simplicity. However, the quality of these controllers depends much on the controller coefficients. In addition, the controller coefficients adjusted to increasing the dynamic response of these controllers make the overshoot increase. This can cause overcurrent and damage power electronic devices. Meanwhile, the HC controller offers the fast response and low overshoot [2]–[7]. However, this HC controller has the switching frequency to vary in a wide range and difficult to control. Therefore, in order to keep the switching frequency constant, the HC controller needs to apply the adaptive hysteresis band as proposed in [6], [8]. This leads to the complex calculation of digital signal processors. In addition, the use of the three independent HC controllers for the three phases makes the switching states difficult to be optimal. This leads the number of switching commutations of the HC controller to increase high. When increasing the hysteresis bandwidth to reduce the switching frequency, the inverter output harmonics increase significantly. The current harmonics of the inverters cause negative effects for the power quality of the power network [9]. In order to ensure the electric energy operation and transmission are safe and stable, the grid codes are promulgated by the electric system operators such as IEEE-929 (2000) [10], IEEE-1547 (2009) [11]-[9] of the United States, IEC 62116 (2005),

IEC 61727 (2007), EN 50160 in Europe, and VDE 0126 (2006) in Germany. In addition, the harmonic limits 519 (2014) in [12] are also applied for grid-connected inverters. Then, the conventional control methods can cause overcurrent for IGBTs due to the high overshoot.

Moreover, the digital control platforms basing on DSPs become very popular due to the semiconductor technology development and suitable for the discrete control. This helps the digital control methods increase advantages. In which, a method basing on the model prediction will promote these benefits. The method of model predictive control (MPC) can completely reject the control loops. However, the MPC in [13] has not been used popularly in the field of grid-connected inverters because of the dependence of the system parameters [14]–[16]. Therefore, this paper proposes a control method of three-phase grid-connected inverters using the model predictive control. Due to its good dynamic response, the HC control method will be described in Section II to make the fundamentals compare with the MPC method. The MPC method is also presented in detail in Section III. The results and discussion in Section IV will show the effectiveness of the MPC method compared with that of the HC one. The harmonics and switching counts are also considered quantitively. In addition, a strategy for decreasing the number of switching commutations is also proposed in this section. This strategy will help inverters reduce the switching loss. Section V will include the advantages of the MPC method.

## II. HYSTERESIS CURRENT CONTROL

A common grid-connected inverter has a structure as Fig. 1. The required active and reactive powers of the system needed to inject into the grid will be calculated according to the reference currents $I_{d\text{-}ref}$ and $I_{q\text{-}ref}$ respectively. A phase-locked loop (PLL) is used to extract the grid voltage angle θ. This angle is used to convert the currents $I_{d\text{-}ref}$ and $I_{q\text{-}ref}$ in the synchronous frame dq into the three phase currents as Fig. 2. In the HC control method, three reference phase currents are compared with three output phase currents of inverter [6], [8] respectively. Thus, there are three HC controllers used in this method.

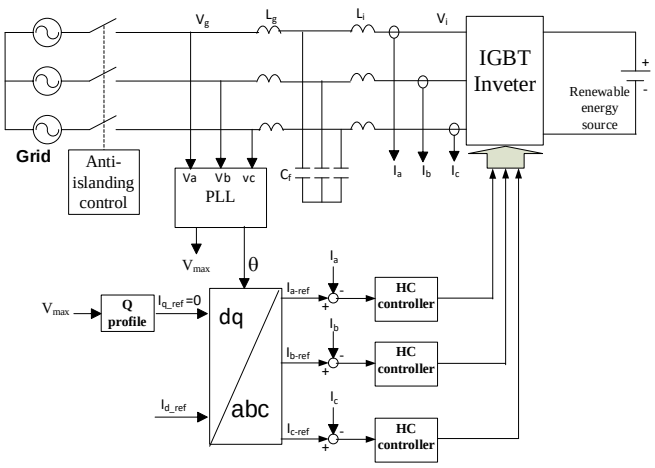


*Fig. 1: Three-phase grid-connected inverter system using the HC controller.*

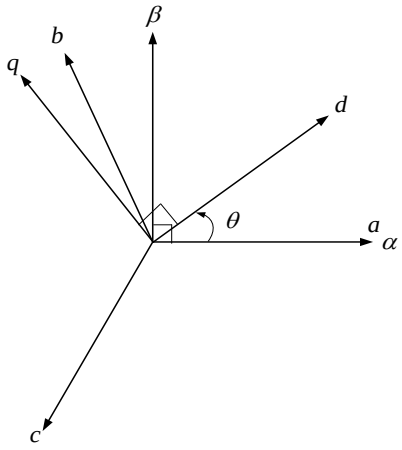


*Fig. 2: Coordinate transformation*

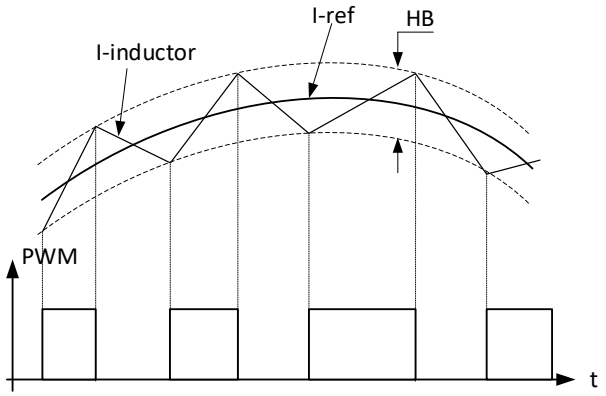


*Fig. 3: The switching principle of the HC controller*

The switching principle of each phase current is showed in Fig. 3. Then, the pulse-width modulation (PWM) depends on the hysteresis bandwidth (HB). The switching frequency is difficult to control. Especially, in the regions of small current value, the switching frequency can

increase highly. To solve this issue, an adaptive hysteresis bandwidth can be used [8], [17]. However, the calculation will be more complex. So, in reality, the fixed HB is often used [7]. A principle model on Matlab/Simulink in Fig. 4, using the HC control method, has a 2-level 3-phase inverter with 6 IGBTs as Fig. 5. The outputs consist eight switching states of 3 phases, Sa, Sb, and Sc.

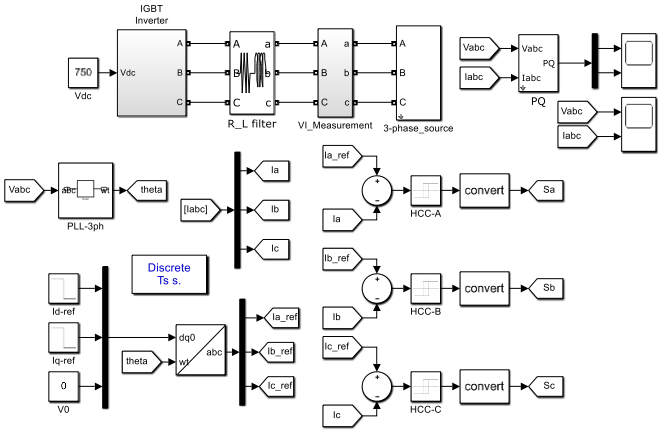


*Fig. 4: Simulink model using the HC controller*

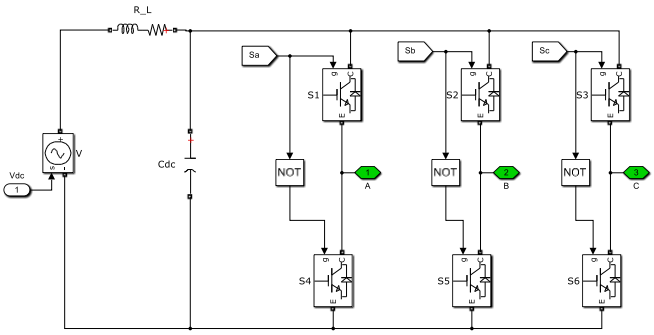


*Fig. 5: 3-phase inverter model*

## III. MODEL PREDICTIVE CONTROL

The space vector modulation and development of DSP help the MPC be popularly applied [18]. Moreover, the control concepts in the MPC are also very intuitive. The principle diagram of the MPC method is showed in Fig. 6 and its operational principle is also showed in Fig. 7. The state space model is described as (1).

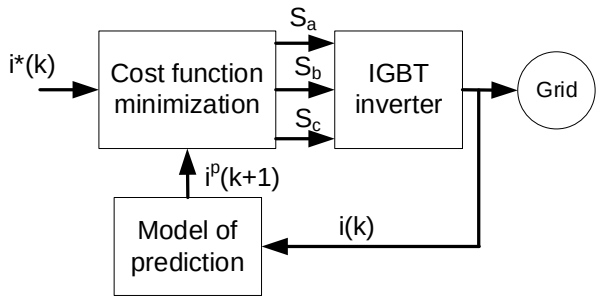


*Fig. 6: The principle model of MPC*

$$\begin{aligned} x(k+1) &= Ax(k) + Bu(k) \\ y(k) &= Cx(k) + Du(k) \end{aligned} \quad (1)$$

Where k is the sample instant. Then, the cost function is described as (2) and represents the expected response of the system. In the 2-level 3-phase inverter, the number of states is defined as (3) and showed in Fig. 8.

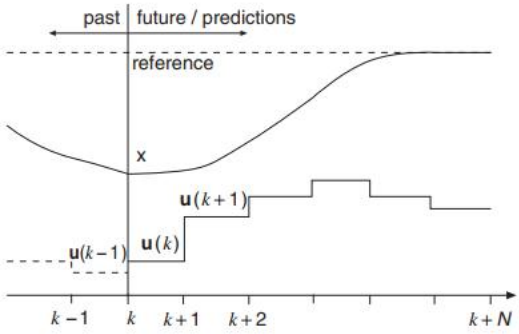


*Fig. 7: The operational principle of MPC*

$$g = f\left(x(k), u(k), ..., u(k+N)\right) \quad (2)$$

$$N = x^y = 2^3 = 8 \quad (3)$$

Then, the cost function of the current control using the MPC will be defined as follows.

$$g = \left|i_\alpha^*(k+1) - i_\alpha^p(k+1)\right| + \left|i_\beta^*(k+1) - i_\beta^p(k+1)\right| \quad (4)$$

Where $i_\alpha^*(k+1)$ and $i_\beta^*(k+1)$ are the real and image of the reference current vector $i^*(k+1)$ to inject into the grid. $i_\alpha^p(k+1)$ and $i_\beta^p(k+1)$ are the real and image of the predictive current $i^p(k+1)$ to inject into the grid at the instant k+1. In order for simplicity, we assume the reference current is unchanged in the sampling cycle Ts. Then, $i^*(k+1)$ is as $i^*(k)$.

*The switching states of IGBTs are defined as follows.*

$$Sa = \begin{cases} 1 & if \quad S1 \quad ON \quad and \quad S4 \quad OFF \\ 0 & if \quad S1 \quad OFF \quad and \quad S4 \quad ON \end{cases} \quad (5)$$

$$Sb = \begin{cases} 1 & if \quad S2 \quad ON \quad and \quad S5 \quad OFF \\ 0 & if \quad S2 \quad OFF \quad and \quad S5 \quad ON \end{cases} \quad (6)$$

$$Sc = \begin{cases} 1 & if \quad S3 \quad ON \quad and \quad S6 \quad OFF \\ 0 & if \quad S3 \quad OFF \quad and \quad S6 \quad ON \end{cases} \quad (7)$$

The phase voltage equations will be defined as

$$V_{aN} = L\frac{di_a}{dt} + Ri_a + V_{ga} + V_{nN}$$
$$V_{bN} = L\frac{di_b}{dt} + Ri_b + V_{gb} + V_{nN}$$
$$V_{cN} = L\frac{di_c}{dt} + Ri_c + V_{gc} + V_{nN} \quad (8)$$

Then, the voltage vector V can be inferred as

$$V = \frac{2L}{3}\frac{d\left(i_a + pi_b + p^2 i_c\right)}{dt} + \frac{2R}{3}\left(i_a + pi_b + p^2 i_c\right) + \frac{2}{3}\left(V_{ga} + pV_{gb} + p^2 V_{gc}\right) + \frac{2}{3}\left(V_{nN} + pV_{nN} + p^2 V_{nN}\right) \quad (9)$$

*Where p is as $e^{j2\pi/3}$. According to the definite of space vector, the grid current and voltage will be defined as follows.*

$$i = \frac{2}{3}\left(i_a + pi_b + p^2 i_c\right) \quad (10)$$

$$e = \frac{2}{3}\left(V_{ga} + pV_{gb} + p^2 V_{gc}\right) \quad (11)$$

And assume that

$$\left(V_{nN} + pV_{nN} + p^2 V_{nN}\right) = V_{nN}\left(1 + p + p^2\right) = 0 \quad (12)$$

Then, the inverter output voltage will be as follows.

$$V = Ri + L\frac{di}{dt} + e \quad (13)$$

The derivative of the current in the discrete domain with the sampling cycle $T_s$ according to the forward Euler method will be as follows.

$$\frac{di}{dt} \approx \frac{i(k+1) - i(k)}{T_s} \quad (14)$$

The predictive current at the time k+1 will be as.

$$i^p(k+1) = \left(1 - \frac{RT_s}{L}\right)i(k) + \frac{T_s}{L}\left(V(k) - \hat{e}(k)\right) \quad (15)$$

Where ê(k) is the estimated grid voltage. The algorithm of the MPC is showed in Fig. 9. Where the weight factor Lamda (λ) is used to consider the reduction of the number of switching commutations. S is calculated as (16) and is the sum of switching commutations and x is the phases A, B, and C respectively.

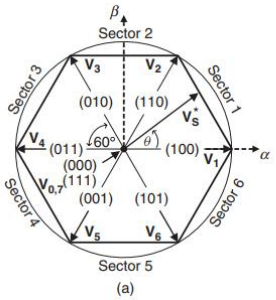


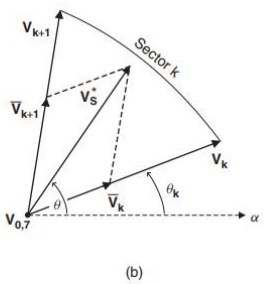


*Fig. 8: The states and principle of space vector*

$$S = \sum_{x=1}^{3}\left|S_x(k+1) - S_x(k)\right| \quad (16)$$

A simulation model on Matlab/Simulink using the MPC is showed in Fig. 9. The dynamic circuit parameters are the same as those of the Fig. 4. In the MPC model, the controller uses the block Matlab function in Simulink.

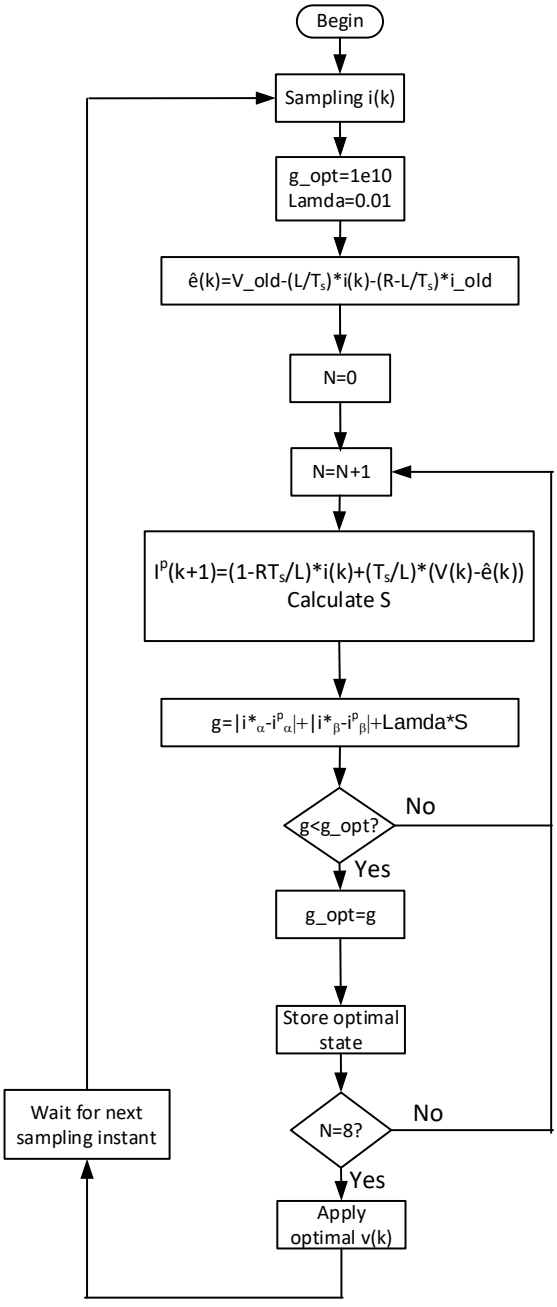


*Fig. 9: Algorithm of the MPC*

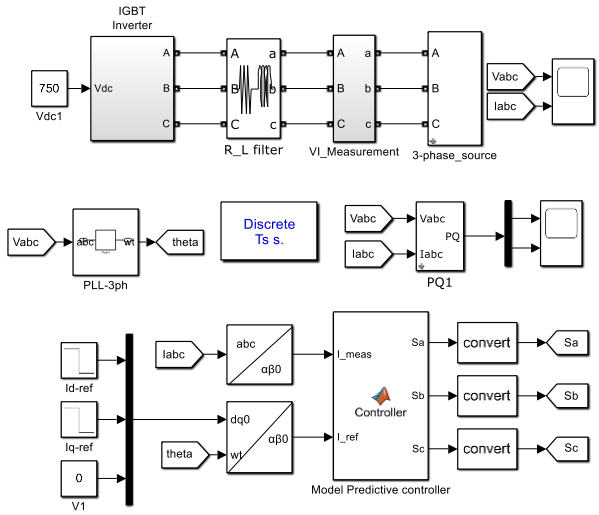


*Fig. 10: Simulink model of the MPC*

## IV. RESULTS AND DISCUSSION

*Table 1. The system parameters*

| Symbol | Description | Value |
|---|---|---|
| $V_g$ | Grid voltage | 3*380 V |
| $f_g$ | Grid frequency | 50 Hz |
| $R_f$ | Filter resistor | 0.001 Ohm |
| $L_f$ | Filter inductor | 7.5 mH |
| $V_{dc}$ | DC voltage | 750 V |
| $T_s$ | Sampling time | 1e-5 s |
| $T_{sd}$ | MPC sampling time | 4e-5 s |
| $\lambda$ | Weight factor | 1e-2 |

The system parameters are showed in Table 1. There are two intervals for survey in this paper. In the first interval, 0-0.4 s, the reference current is changed in the step, $I_{d\text{-}ref}$ as 40 A, and in the final interval, 0.4 0.6 s, $I_{d\text{-}ref}$ as 20 A.

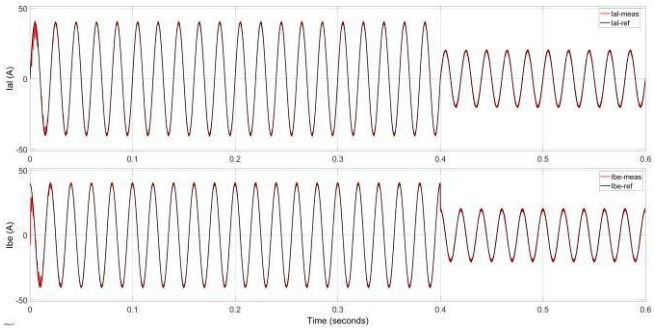


*Fig. 11: Current responses of the HC*

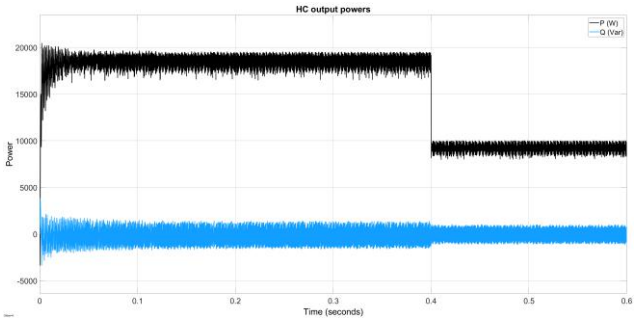


*Fig. 12: Power response of the HC*

The reference current $I_{q\text{-}ref}$ is always as 0. This means that the only active power is injected into the grid.

The simulation results in Figs. 11-14 have showed the current and power responses of the HC method. These results also showed the settling time and overshoot are very small.

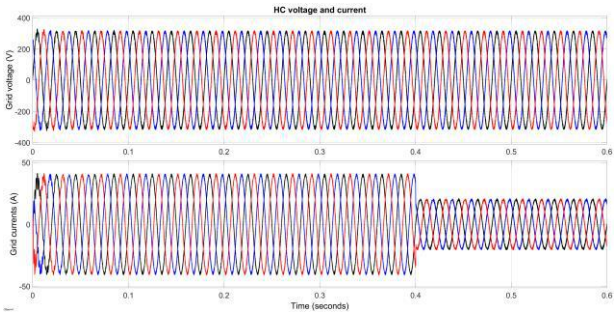


*Fig. 13: Voltage and current response of the HC*

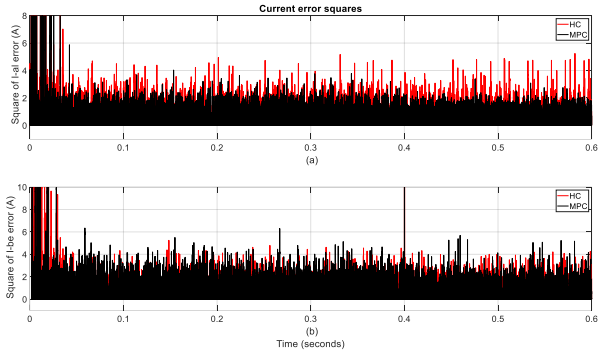


*Fig. 14: Squares of current errors of the HC and MPC*

However, the current steady state error of the HC method is significantly high. This is showed clearly in Fig. 14(a), in which the squares of the current errors of the HC method in the red are higher than 5 A. While those of the MPC one in the black are always lower than 4 A. The phase A current harmonics of the two methods are also measured at the final fundamental period of each interval and showed in Table 2.

*Table 2. Comparison of methods*

| Time (s) | 0-0.04 | | 0.4-0.6 | |
|---|---|---|---|---|
| Method | $THD_I$ (%) | $I_{peak\_fund}$ (A) | $THD_I$ (%) | $I_{peak\_fund}$ (A) |
| HC | 2.42 | 39.72 | 4.79 | 19.76 |
| MPC | **2.26** | **39.96** | **4.55** | **20** |

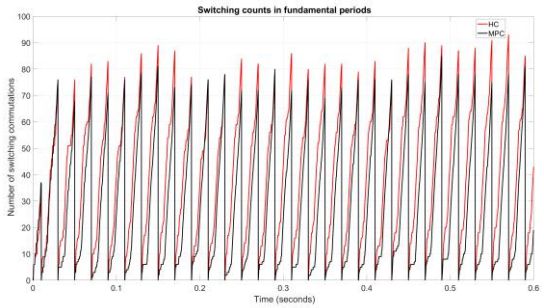


*Fig. 15: Switching counts of the HC and MPC with λ=0*

The current total harmonic distortions of the HC control are 2.42 % and 4.79 %. These values are higher than those of the MPC one, 2.26 % and 4.55 % respectively. Moreover, the fundamental current magnitude of the MPC, as 39.96 A and 20 A, are higher than those of the HC one, as 39.72 A and 19.76 A respectively. This helps increase the generation efficiency of the inverters.

In addition, the number of switching commutations in each fundamental period in Fig. 15, with λ=0, has showed that the switching counts of the MPC in the black are lower than 80. While those of the HC method in the red are always higher than 80.

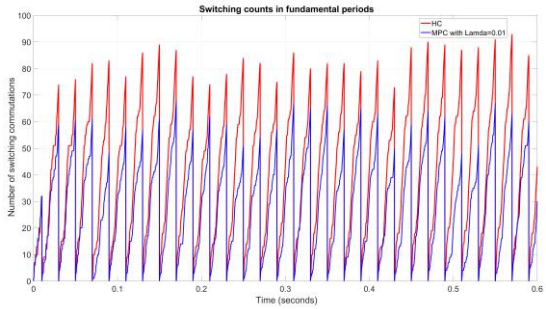


*Fig. 16: Switching counts of the HC and MPC with λ=0.01*

When considering the reduction of switching count with the weight factor λ=0.01, the number of switching commutations of the MPC, in the blue in Fig. 16, is always lower than 65. Although the number of switching commutations of the MPC is lower than those of the HC, the current THD of the MPC is still lower than that of the HC in Fig. 17.

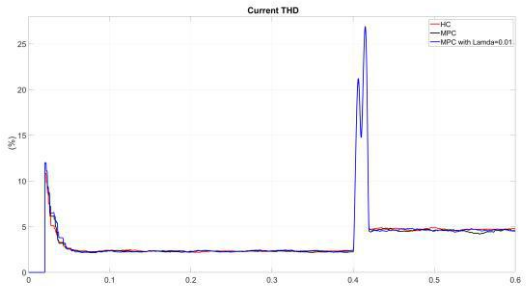


*Fig. 17: Current THD of HC and MPC*

## V. CONCLUSION

This paper has presented a method using the model predictive control for three-phase grid-connected inverters. An algorithm for reducing the number of switching commutations is also proposed by including the weight factor in the cost function of the MPC. The simulation models of the MPC and HC methods built on Matlab/Simulink are used for verifying the proposed algorithm.

The performance of the proposed MPC method has also been validated when comparing the simulation results of the MPC with those of the HC one. The current harmonics, the number of switching commutations, overshoot, and settling time are also considered quantitively.

## ACKNOWLEDGEMENTS

This work belongs to the project grant No: T2020-21TĐ funded by Ho Chi Minh City University of Technology and Education, Vietnam.

## REFERENCES

[1] R. Teodorescu, M. Liserre, and P. Rodriguez, *Grid Converters for Photovoltaic and Wind Power Systems*. 2011.

[2] S. Lakhimsetty, V. S. P. Satelli, R. S. Rathore, and V. T. Somasekhar, "Multilevel Torque Hysteresis-Band based Direct-Torque Control Strategy for a Three- Level Open-End Winding Induction Motor Drive for Electric Vehicle Applications," *IEEE J. Emerg. Sel. Top. Power Electron.*, vol. 7, no. 3, pp. 1969–1981, 2019.

[3] S. Madanzadeh, A. Abedini, A. Radan, and J.-S. Ro, "Application ofquadratic linearization state feedback control with hysteresis reference reformer to improve the dynamic response of interior permanent magnet synchronous motors," *ISA Trans. J.*, vol. 99, pp. 167–190, 2020.

[4] Y. Xue *et al.*, "Vector-Based Model Predictive Hysteresis Current Control for Asynchronous Motor," *IEEE Trans. Ind. Electron.*, vol. 66, no. 11, pp. 8703–8712, 2019, doi: 10.1109/TIE.2018.2886754.

[5] S. J, A. S, and R. Ramchand, "Current Error Space Vector Based Hysteresis Controller for VSI Fed PMSM Drive," *IEEE Trans. Power Electron.*, vol. 35, no. 10, pp. 10690–

10699, 2020.

[6] A. Narendran and R. Sureshkumar, "Hysteresis-controlled - landsman converter based multilevel inverter fed induction-motor system using PIC," *Microprocess. Microsyst.*, vol. 76, 2020.

[7] R. Viswadev, A. M, V. V. Ramana, B. Venkatesaperumal, and S. Mishra, "A Novel AC Current Sensorless Hysteresis Control for Grid-tie Inverters," *IEEE Trans. Circuits Syst. II Express Briefs*, vol. 67, no. 11, pp. 2577–2581, 2020.

[8] M. Kale, E. Ozdemir, and Electrical, "An adaptive hysteresis band current controller for shunt active power filte," *Electr. Power Syst. Res.*, vol. 73, pp. 113–119, 2005.

[9] J. C. Das, "Power system harmonics," in *Power System Harmonics and Passive Filter Designs*, New Jersey: John Wiley & Sons, 2015, pp. 11–16.

[10] IEEE, "IEEE Recommended Practice for Utility Interface of Photovoltaic (PV) Systems," *IEEE Std 929-2000*. 2000, doi: 10.1109/IEEESTD.2000.91304.

[11] IEEE Standard, "IEEE Application Guide for IEEE Std 1547(TM), IEEE Standard for Interconnecting Distributed Resources with Electric Power Systems," *IEEE Std 1547.2-2008*, no. April, pp. 1–217, 2009, doi: 10.1109/IEEESTD.2008.4816078.

[12] J. Cheng, CEng, CEM, CEA, and CMVP, "IEEE Standard 519-2014," *Schneider Electric*. p. 50, 2014.

[13] M. B. Shadmand, R. S. Balog, and H. Abu-Rub, "Model predictive control of PV sources in a smart DC distribution system: Maximum power point tracking and droop control," *IEEE Trans. Energy Convers.*, vol. 29, no. 4, pp. 913–921, 2014, doi: 10.1109/TEC.2014.2362934.

[14] J. Yuan, Y. Yang, P. Liu, and F. Blaabjerg, "Model Predictive Control of An Embedded Enhanced-Boost Z-Source Inverter," *2018 IEEE 19th Work. Control Model. Power Electron. COMPEL 2018*, vol. 2, no. 3, pp. 1–6, 2018, doi: 10.1109/COMPEL.2018.8459954.

[15] J. M. C. Geldenhuys, H. Du Toit Mouton, A. Rix, and T. Geyer, "Model predictive current control of a grid connected converter with LCL-filter," *2016 IEEE 17th Work. Control Model. Power Electron. COMPEL 2016*, 2016, doi: 10.1109/COMPEL.2016.7556734.

[16] D. Sankar and C. A. Babu, "Model predictive control of five level cascaded H bridge multilevel inverter for photovoltaic system," *Proc. 2016 Int. Conf. Cogener. Small Power Plants Dist. Energy, ICUE 2016*, no. September, pp. 14–16, 2016, doi: 10.1109/COGEN.2016.7728946.

[17] P. Ghani, A. A. Chiane, and H. M. Kojabadi, "An adaptive hysteresis band current controller for inverter base DG with reactive power compensation," in *PEDSTC 2010 - 1st Power Electronics and Drive Systems and Technologies Conference*, 2010, pp. 429–434, doi: 10.1109/PEDSTC.2010.5471776.

[18] J. Rodriguez and P. Cortes, *Predictive control of power converters and electrical drives*. John Wiley & Sons, Ltd., Publication, 2012.